Laboratory Investigation (2014) 94, 806–817

Mouse models of mantle cell lymphoma, complex changes in gene expression and phenotype of engrafted MCL cells: implications for preclinical research

Magdalena Klanova[1,2], Tomas Soukup[3], Radek Jaksa[4], Jan Molinsky[1,2], Lucie Lateckova[1,2], Bokang CL Maswabi[1], Dana Prukova[1], Jana Brezinova[5], Kyra Michalova[5], Petra Vockova[1,2], Francisco Hernandez-Ilizaliturri[6], Vojtech Kulvait[1], Jan Zivny[1], Martin Vokurka[1], Emanuel Necas[1], Marek Trneny[2,5] and Pavel Klener[1,2]

Mantle cell lymphoma (MCL) is an aggressive type of B-cell non-Hodgkin lymphoma (NHL) associated with poor prognosis. Animal models of MCL are scarce. We established and characterized various *in vivo* models of metastatic human MCL by tail vein injection of either primary cells isolated from patients with MCL or established MCL cell lines (Jeko-1, Mino, Rec-1, Hbl-2, and Granta-519) into immunodeficient NOD.Cg-*Prkdc*^{scid} *Il2rg*^{tm1Wjl}/SzJ mice. MCL infiltration was assessed with immunohistochemistry (tissues) and flow cytometry (peripheral blood). Engraftment of primary MCL cells was observed in 7 out of 12 patient samples. The pattern of engraftment of primary MCL cells varied from isolated involvement of the spleen to multiorgan infiltration. On the other hand, tumor engraftment was achieved in all five MCL cell lines used and lymphoma involvement of murine bone marrow, spleen, liver, and brain was observed. Overall survival of xenografted mice ranged from 22 ± 1 to 54 ± 3 days depending on the cell line used. Subsequently, we compared the gene expression profile (GEP) and phenotype of the engrafted MCL cells compared with the original *in vitro* growing cell lines (controls). We demonstrated that engrafted MCL cells displayed complex changes of GEP, protein expression, and sensitivity to cytotoxic agents when compared with controls. We further demonstrated that our MCL mouse models could be used to test the therapeutic activity of systemic chemotherapy, monoclonal antibodies, or angiogenesis inhibitors. The characterization of MCL murine models is likely to aid in improving our knowledge in the disease biology and to assist scientists in the preclinical and clinical development of novel agents in relapsed/refractory MCL patients.
Laboratory Investigation (2014) **94,** 806–817; doi:10.1038/labinvest.2014.61; published online 26 May 2014

KEYWORDS: experimental therapy; immunodeficient mice; lymphoma microenvironment; mantle cell lymphoma; mouse xenograft model

Mantle cell lymphoma (MCL) is an aggressive type of B-cell non-Hodgkin lymphoma (NHL) characterized by the chromosomal translocation t(11;14)(q13;q32) leading to overexpression of cyclin D1.[1] Apart from this canonical aberration, MCL may harbor a large number of recurrent cytogenetic changes that further deregulate cell cycle machinery (for example, deletion of 9p21 (CDKN2A) and amplification of 12q13 (CDK4)) or interfere with cellular response to DNA damage (for example, alterations of 11q22-q23 (ATM), 17p13 (TP53) and overexpression of MDM2).[2–5] MCL is associated with poor prognosis.[6,7] In order to improve the outcome of MCL patients, the rational development and preclinical/clinical testing of new agents are necessary. Reliable and reproducible *in vivo* models of MCL are thus urgently needed. *In vivo* models have several advantages over *in vitro* approaches. For example, they enable the study of MCL biology in its microenvironment, including engraftment, growth rate, spread patterns, or tumor associated neovascularization.

[1]First Faculty of Medicine, Institute of Pathological Physiology, Charles University in Prague, Prague, Czech Republic; [2]First Department of Medicine, Clinical Department of Hematology of the General University Hospital, Charles University in Prague, Prague, Czech Republic; [3]Medical Faculty Hradec Kralove, Institute of Histology and Embryology, Charles University, Prague, Czech Republic; [4]First Faculty of Medicine, Institute of Pathology, Charles University in Prague; [5]Institute of Hematology and Blood Transfusion, Prague, Czech Republic and [6]Department of Medical Oncology and Immunology, Cancer Cell Center, Roswell Park Cancer Institute, Buffalo, NY, USA

Correspondence: Dr M Klanova, MD, First Faculty of Medicine, Institute of Pathological Physiology, Charles University in Prague, U Nemocnice 5, Prague 2, 12853, Czech Republic.

E-mail: magdalena.klanova@seznam.cz

Received 20 September 2013; revised 24 March 2014; accepted 28 March 2014

In addition, *in vivo* models are preferable for the testing of agents that cannot be reliably tested *in vitro* (for example, monoclonal antibodies, immunomodulatory drugs, pro-drugs, inhibitors of B-cell receptor signaling, or inhibitors of angiogenesis). Mouse models of MCL reported in the literature include two large groups: (1) genetically engineered mice predisposed to develop a MCL-like disease and (2) immunodeficient mice capable of bearing human MCL xenografts.[8–11] Recently, characterization of a mouse xenograft model using primary MCL cells was reported; however, it was unfortunately technically demanding and difficult to implement.[11] Currently, the most widely used MCL xenograft model utilizes the subcutaneous injection of established MCL cell lines into immunodeficient mice.[12–15]

To further improve on the current available MCL mouse models, we established and characterized several reproducible metastatic mouse models of human MCL by the inoculation of human primary MCL cells or MCL cell lines (Jeko-1, Mino, Rec-1, Granta-519, and Hbl-2) via tail vein injection (i.v.) into an immunodeficient mice NOD.Cg-*Prkdc*^{scid} *Il2rg*^{tm1Wjl}/SzJ (non-obese diabetic, interleukin-2 receptor gamma common chain null), commonly referred to as NOD-SCID-gamma (NSG) mice. We demonstrated that MCL cells obtained *ex vivo* from various infiltrated murine organs displayed distinct changes in gene expression profile (GEP), immunophenotype, and sensitivity to cytotoxic agents compared with *in vitro* growing MCL cells. Our findings suggest that engraftment of MCL cells into immunodeficient mice leads to clonal selection and illustrate the complex interaction between lymphoma cells and its host. Moreover, given the different responses to standard chemotherapy agents observed between MCL cells and MCL isolated following *in vivo* engraftment our work further stress the need to use both *in vitro* and *in vivo* preclinical models in the evaluation of novel agents for B-cell lymphoma patients.

MATERIALS AND METHODS

MCL Cell Lines

MCL cell lines Jeko-1, Rec-1, and Granta-519 were obtained from the German Collection of Microorganisms and Cell Cultures (DSMZ). The Mino cell line was obtained from American Tissue Culture Collection (ATCC), and the Hbl-2 cell line was a kind gift from Professor Martin Dreyling (University of Munich, Munich, Germany).

Primary MCL Cells

Primary MCL cells were obtained from the peripheral blood, bone marrow (BM), lymph node, or pleural effusion of MCL patients. Mononuclear cells were isolated by the standard Ficoll–Hypaque gradient centrifugation, and frozen in heat inactivated fetal bovine serum supplemented with 10% dimethyl sulfoxide (DMSO).

Samples were obtained after informed consent according to the Declaration of Helsinki. This work was approved by the Ethics committee of the General University Hospital in Prague.

Immunodeficient Mice

The NOD.Cg-*Prkdc*^{scid} *Il2rg*^{tm1Wjl}/SzJ mice (referred to as NSG mice) were purchased from The Jackson Laboratory (Bar Harbor, Maine, USA). All animals were housed and maintained in a pathogen-free environment in individually ventilated cages and provided with sterilized food and water. The experimental design was approved by the institutional animal care and use committee.

Xenograft Experiments Using Primary MCL Cells

Eight- to twelve-week-old female NSG mice were used for all experiments. On day 1 the mice were sublethally irradiated (2.5 Gy) and subsequently inoculated via tail vein injection with freshly thawed primary MCL cells ($10–80 \times 10^6$). Upon the development of hint-leg paralysis or generalized inability to thrive, animals were euthanized by cervical dislocation. Mice that showed no signs of lymphoma engraftment were killed 60 days following tumor cell inoculation. Selected murine organs were subjected to immunohistochemical (IHC) analysis to assess organ infiltration with human cells (see in detail further).

Xenograft Experiments Using MCL Cell Lines

The mice were injected with 1×10^6 MCL cells (Granta-519, Hbl-2, and Jeko-1) or 10×10^6 MCL cells (Rec-1 and Mino) via tail vein injection. Two animals from each cohort were killed at four different time points (designated T1, T2, T3, and T4). T1 was set as the midpoint between the day of tumor inoculation (Day 0) and the estimated overall survival (OS). OS was defined as the time between tumor cell inoculation (Day 0) and the time of development of limb paralysis (T4). T2 and T3 were set in between of the T1 and T4 time points so that they represented one-third and two-thirds of the interval between T1 and T4, respectively. At T4 time point, peripheral blood samples were collected following anesthesia with ketamine–xylazin by retro-orbital exsanguination and before euthanasia. Then, red cells were lyzed using a lysis buffer (BioLegend, USA) and the samples were submitted to flow cytometric analysis (see section Flow cytometry analysis).

IHC Analysis

Once the animals reached T4, necropsy studies were performed. Murine organs were removed, fixed in 4% formalin for 7 days, cut into tissue blocks, embedded in paraffin, and sectioned into transversal and longitudinal 6–7 μm thick slices. Sections were stained with hematoxylin and eosin, Masson's blue trichrome, and Gömöri impregnation.[16] IHC staining for human CD45 (2B11, PD7/26), CD20 (L26), cyclin D1 (DSC-6), Ki-67/MIB1 (DakoCytomation), and CD3 (SP7) (Neomarkers) was performed. Antigen retrieval was carried out in citrate buffer solution (0.291% sodium

citrate, 0.05% Tween 20, pH 6.0) using microwave for 3×5 min. Standard ABC (Avidin Biotin Complex) method was used for the detection with 3,3′-Diaminobenzidine. Mayer's hematoxylin was used for counterstaining. Images were obtained using Olympus BX51 equipped with a DP25 digital camera. Data were analyzed with the Image-Pro Plus 5.1 software within 20 samples from different organ areas (40 visual fields were evaluated per sample). Experiments were carried out in duplicates for each time point (two mice for each time point).

Detection of EBV DNA and RNA

EBV-encoded RNA (EBER) was detected by *in situ* hybridization on formalin-fixed, paraffin-embedded tissue sections using EBER peptide nucleic acid (PNA) Probe/Fluorescein and PNA ISH Detection Kit (DakoCytomation). It was carried out at the Institute of Pathology of the First Faculty of Medicine, Charles University in Prague, according to the standard operating protocol.

DNA was isolated according to the manufacturer's instructions from 200 μl of cell culture supernatant using High Pure Viral Nucleic Acid Kit (Roche Diagnostics GmbH, Germany). EBV DNA was measured with quantitative real-time PCR (LightCycler EBV Quant Kit, Cepheid AB, Sweden) and run on a Light Cycler 2.0 instrument (Roche Diagnostics GmbH, Germany). The test was performed according to the original manufacturer's protocol.

Ex Vivo Isolation of MCL Cells

The murine organs were homogenized using 45 μM cell strainers (Becton Dickinson). Bone marrow was flushed from murine femurs with 3 ml of sterile PBS into a sterile container and passed through the 45-μM cell strainer. Human MCL cells were isolated from homogenized murine organs (BM, liver (L), spleen (S), lymph node-like tumors (T)) by magnetic cell sorting using an anti-human-CD45 micro beads (Miltenyi Biotec) at T4 time point. The purity of MCL population after sorting was $>95\%$ in all cases as verified using flow cytometry. MCL cells cultured in parallel *in vitro* served as controls (CTRL cells) and were processed in the same way (that is, they were sorted on magnetic columns using anti-CD45 microbeads) to eliminate any potential bias caused during the magnetic cell sorting. *Ex vivo* obtained CD45-sorted cells were either directly used for experiments (designated BM, S, L, or T) or they were recultured for 14 days *in vitro* (designated BM-EX, S-EX, L-EX, and T-EX), after which they were again CD45-sorted and used for experiments.

GEP

Mino and Jeko-1 cell lines were used for GEP studies. Total mRNA was isolated from *in vitro* cultured or *ex vivo*-sorted MCL cells in RNA *later* solution using RNeasy Mini Kit (Qiagen, Hilden, Germany). Quality of RNA was assessed using the Agilent 2100 Bioanalyzer (Agilent Technology). Extracted RNA was amplified using the Illumina RNA Amplification Kit (Ambion). Amplified RNA was hybridized to the IlluminaHumanRef-12 BeadChips (Mino) and IlluminaHumanRef-8 Bead Chips (Jeko-1). Differences in gene expressions between MCL cells obtained from different murine organs were investigated. Data analysis was performed in R-software[17] using Bioconductor[18] repository packages. Particularly, we used the bead array package for data extraction.[19] We further analyzed Illumina expression data on the level of unsummarized beads. We performed quantile normalization and *t*-test to find significantly differently expressed mRNAs between two states of our interest. A multiple testing correction was performed using the Benjamini and Hochberg method (Benjamini and Hochberg, 1995). The filtered group of genes with fold change greater/lower than ± 1.2, and adjusted *P*-values <0.05 were annotated and arranged into biologically relevant categories using The Database for Annotation, Visualization and Integrated Discovery (DAVID, http://david.abcc.ncifcrf.gov).

Flow Cytometry Analysis

Flow cytometry was performed on BD FACS Canto II and evaluated using FCS express software (version 3). The following directly conjugated antibodies were used in this study: an anti-human allophycocyanin (APC)-conjugated anti-CD44 (MEM-85), a phycoerythrin (PE)-conjugated anti-CD45R (MEM-28) (Exbio, Czech Republic), a PE-conjugated anti-CD31 (PECAM-1; WM59), a peridinin-chlorophyll protein Cyanine 5.5 (PerCP-Cy5.5)-conjugated anti-CD45 (2D1), a fluorescein isothiocyanate-labeled anti-CD20 (2H7), an APC-labeled anti-CD184 (CXCR4)-APC (12G5), a PE-conjugated anti-CD197 (CCR7; G043H7), and PE-conjugated anti-podoplanin (NC-08; BioLegend).

Cell Proliferation Assays

MCL cells were plated at a cell density of 5000 cells per 0.3 ml and exposed to the following chemotherapy agents: cytarabine or cisplatin. Cell proliferation was measured using the WST-8-based Quick Cell Proliferation Assay Kit (BioVision) according to the manufacturer's instructions.

Re-Transplantation Experiments

MCL cells were obtained from the BM of NSG mice inoculated with 10×10^6 Mino or 1×10^6 Jeko-1 cells (primary recipients). MCL purification was achieved using CD45 microbeads. Subsequently, isolated MCL cells were inoculated via tail vein injection into additional non-radiated NSG mice (secondary recipients). NSG mice inoculated with *in vitro* growing MCL cells (CTRL cells) were used as controls.

Similar experiments were performed using cells isolated from MCL patients. For these experiments, primary MCL cells were isolated from infiltrated organs (spleen) of NSG mice (primary recipients). No cell sorting was used; instead, unsorted MCL cells were obtained *ex vivo* from the infiltrated spleen by passing the spleen through the 45-μM cell strainer,

washed in PBS, and injected into sublethally irradiated NSG mice (secondary recipients).

Experimental Single-Agent Therapy of MCL Xenografts

To study the effects of therapeutic interventions in our *in vivo* models, NSG mice were inoculated with 10×10^6 Mino, 1×10^6 Jeko-1, or 10×10^6 NEMO cells and divided into several treatment cohorts (five to eight animals/cohort). Treatment started 5 days post inoculation and continued until T4. Control group received sterile PBS. Treatment groups received the following single-agent treatments: (1) cyclophosphamide (3 mg/dose) once weekly, (2) gemcitabine (10 mg/dose) once weekly, (3) fludarabine (1 mg/dose) for 3 consecutive days every week, (4) temsirolimus (1 mg/dose) once weekly, (5) bortezomib (25 μg/dose) twice weekly, (6) rituximab (0.3 mg/dose) twice weekly, (7) bevacizumab (0.3 mg/dose) twice weekly, (8) lenalidomide (1 mg/dose) daily on working days until T4. All agents were administered intraperitoneally (i.p.). Differences in survival between treatments groups were evaluated using Kaplan–Meier survival estimates, which were set-up using Graph-Pad Prism software.

RESULTS

Mouse Models of Human MCL Using Primary MCL Cells

Primary MCL cells ($n = 12$) were isolated from the peripheral blood (PB, $n = 8$), PB and BM ($n = 2$), involved lymph node ($n = 1$) or pleural effusion (PE) ($n = 1$) of MCL patients. Most of the patients presented with the classic variant MCL ($n = 8$). In addition, MCL cells were isolated from pleomorphic ($n = 1$) or blastoid variant ($n = 3$) MCL. Cells were isolated from previously untreated patients ($n = 10$) or at the time of relapse ($n = 2$). Most patients had high MCL International Prognostic Index (MIPI) score ($n = 11$) and had adverse cytogenetics defined as either deletion of TP53 or deletion of ATM ($n = 9$). Engraftment of cyclin D1+ cells was observed in 7 out of 12 patient-derived cell suspensions injected into NSG mice (Table 1, Figure 1). Engraftment was observed across all three morphological variants, including classic ($n = 4/8$), pleomorphic (1/1), or blastoid variant (2/3) MCL. With the exception of cells isolated from VFN-1 patient, all detectable engraftments of cyclin D1+ MCL cells were observed in the spleen of NSG mice. The extent of splenic infiltration by MCL cells (cyclin D1+ cells) and their proliferation rate (Ki-67+ cells) were variable (Figure 1). Inoculation via tail vein injection of MCL cells isolated from case VFN-1 resulted in the diffuse infiltration by cyclin D1+ cells in the spleen, BM, liver, and kidneys (but not central nervous system (CNS)). Apart from VFN-1, xenotransplantation of two primary MCL samples (VFN-4 and VFN-10) resulted in significant infiltration of the spleen by cyclin D1+/Ki-67+ MCL cells (Figure 1b) with no IHC signs of involvement of the liver or BM. Inoculation of NSG mice with primary tumor cells isolated from four patients (cases VFN-3, VFN-6, VFN-7, and VFN-8) was associated with splenic engraftment of CD45+ cells, composed of cyclin D1+, CD20+/cyclin D1−, and CD3+ cells (Figure 1c). Of interest, inoculation of NSG mice with primary tumor cells isolated from patients VFN-2, VFN-11, and VFN-12 resulted in the engraftment of cyclin D1/CD20+/EBER+

Table 1 Primary MCL cells

Patient	Age	Gender	Histological variant	Cytogenetic aberrations	MIPI	Disease status	Sample origin	Number of cells ($\times 10^6$) injected per mouse
VFN-1	64	F	Blastoid	Plus ATM	8.5	1	PB	40
VFN-2	68	M	Blastoid	del 13q34, del ATM, del P53, del CDKN2A, MYC breakage	8.5	0	PB	10
VFN-3	76	M	Blastoid	Monosomy 9 and 13, del ATM	8.5	0	PB + BM	20
VFN-4	70	F	Classic	del 13q34, del ATM, del P53, del CDKN2A	9.1	0	PB + BM	25
VFN-5	46	F	Classic	del 13q14, monosomy 9, del P53, del of CDKN2A	7.5	0	PB	20
VFN-6	58	M	Classic	del 13q14, del 13q34, del ATM, MYC gain	7.6	0	PB	15
VFN-7	56	M	Classic	Monosomy 13, del ATM, del P53, del CDKN2A	8.2	0	PB	40
VFN-8	64	F	Classic	NA	6.8	0	PB	30
VFN-9	79	F	Classic	Normal karyotype	7.6	0	PB	40
VFN-10	64	F	Pleomorphic	del ATM, del P53	8.5	0	PB	80
VFN-11	48	M	Classic	Monosomy 17, del ATM	5.4	0	LN	20
VFN-12	74	M	Classic	del 13q34, monosomy 3 and 9, del ATM, del P53, MYC gain	7.1	1	PE	50

Abbreviations: BM, bone marrow; Disease status (0 = at diagnosis, 1 = at relapse); F, female; LN, lymph node; M, male; MCL, mantle cell lymphoma; MIPI, Mantle cell lymphoma International Prognostic Index; PB, peripheral blood; PE, pleural effusion.

cells (Figure 1d). Quantitative real-time PCR of EBV DNA of the *ex vivo* cultured cells obtained from the infiltrated murine spleen of NSG mice inoculated with either VFN-2, VFN-11, or VFN-12 cells confirmed the presence of EBV DNA. No infiltration of the CNS was detected using IHC analysis in any of the NSG mice inoculated with primary tumor cells isolated from 12 MCL patients. Re-transplantation of the engrafted primary MCL cells was carried out only in the case of VFN-1 sample, namely owing to sufficient numbers of the MCL cells obtained *ex vivo* from the infiltrated murine spleen. However, as the engrafted cells were no longer *stricto senso* primary MCL cells originally contained in the VFN-1 sample, but MCL cells engrafted in the murine tissues, we designated them as NEMO cells. We clearly demonstrated that NEMO cells readily re-engrafted into secondary recipients upon tail vein injection. OS of mice xenografted with 10×10^6 per mouse NEMO cells was significantly shorter compared with the survival of mice xenografted with 40×10^6 million per mouse VFN-1 cells (30.9 ± 5.9 *vs* 61.3 ± 6.8, $P < 0.05$). IHC analysis of NEMO-xenografted mice confirmed the diffuse infiltration of the spleen, BM, liver, and kidneys with cyclin D1+ NEMO cells (Supplementary Figure 1).

Mouse Models of Human MCL Using Established MCL Cell Lines

Engraftment was achieved after xenotransplantation of all five MCL cell lines. The median OS of the xenografted mice was 22 ± 1 days for Granta-519, 30 ± 1.4 days for Hbl-2, 37.3 ± 5.1 days for Jeko-1, 53.5 ± 2 days for Mino, and 53.8 ± 3.4 days for Rec-1 cells. A shared IHC finding in all MCL-bearing animals was the gradually increasing lymphoma infiltration of the BM, spleen, and liver (Figure 2, Supplementary Figure 2, Table 2a) over time. Whereas involvement of the CNS was observed in animals injected with all five MCL cell lines, infiltration of the PB and kidneys was variable (Table 2b). Animals inoculated with Jeko-1 and Rec-1 cells often developed enlargement of the ovaries due to lymphoma infiltration (Figure 2b, Supplementary Figure 2b). Interestingly, mice engrafted with Mino cells frequently developed lymph node-like tumors in the axillary and submandibular regions, or 'extranodal' tumors (intra-abdominal, intra-orbital, or subcutaneous). In addition, mice with bulky intra-abdominal tumors often had malignant ascites (confirmed by FACS, data not shown). IHC analysis of the enlarged submandibular tumor by Gömöri impregnation revealed collagen 3-rich lymph node-like structure composed predominantly of human MCL B cells (Figure 2a). Mice injected with Hbl-2 cells typically developed hint-leg paralysis at T4 (Figure 2c). Signs of terminal disease (weight loss and generalized inability to thrive) were observed in mice injected with Granta-519, Jeko-1, Mino, and Rec-1 cell lines by T4. The extent of infiltration of murine tissues with all five MCL cell lines during T1–T4 time points are given in Table 2. Weights of the murine spleen and liver at T4 correlated with the extent of organ infiltration and are given in Table 2b.

GEP Changes of *Ex Vivo* Obtained MCL Cells when Compared with *In Vitro* growing Cell Line Controls

GEP of MCL cells obtained *ex vivo* from different murine organs (BM, S, L, and T) clustered together and displayed complex GEP changes compared with *in vitro* growing controls (CTRL; Figure 3a). Interestingly, GEP signature of *ex vivo* MCL cells isolated from NSG mice cultured for 14 days *in vitro* reverted to the original MCL *in vitro* signature (Figure 3a). In addition, the filtered group of genes with fold change greater than 1.2 and adjusted *P*-value < 0.05 were annotated and arranged into biologically relevant categories using the DAVID database. B-cell receptor signaling (19 genes) and JAK-STAT signaling (29) pathways belonged to the most upregulated gene sets (out of 16, $P < 0.05$) in BM compared with CTRL Mino cells. B-cell receptor signaling (26 genes), chemokine signaling (40), leukocyte transendothelial migration (28), mammalian target of rapamycin signaling (14), and cell cycle (24) were among the most upregulated signaling pathways/gene signature sets (out of 30, $P < 0.05$) in BM compared with CTRL Jeko-1 cells. The oxidative phosphorylation gene set was the most downregulated group of genes (out of 15) in Jeko-1 BM cells (46 genes, $P < 0.05$), and the second most downregulated one (out of 20) in Mino BM cells (55 genes, $P < 0.05$) compared with CTRL cells.

Immunophenotype Changes Following *In Vivo* Engraftment of MCL Cells

Flow cytometry analysis of Mino cells isolated from a lymph node-like tumor (T) in NSG mice compared with CTRL Mino cells demonstrated the upregulation of CD44 and a downregulation of CCR7 and podoplanin. In addition, flow cytometry analysis of Mino cells obtained from the infiltrated BM in NSG mice compared with CTRL Mino cells demonstrated cell surface downregulation of CCR7, CXCR4, CD44, and podoplanin (Figure 3b). The degree of CCR7 downregulation in the BM compartment was more profound than that in the lymph node compartment (Figure 3b). Flow cytometry analysis of the Jeko-1 cells obtained from NSG mice (BM and spleen) compared with CTRL Jeko-1 cells grown *in vitro* demonstrated an upregulation of CD31 and CD44 and a downregulation of CCR7, CXCR4, and podoplanin (Figure 3b). *Ex vivo* obtained MCL cells recultured for 2 weeks *in vitro* (BM-EX, T-EX, and S-EX) had immunophenotype profiles similar to CTRL cells (data not shown).

Sensitivity to Cytotoxic Agents of MCL Subpopulations Obtained *Ex vivo* from Different Murine Organs Compared with *In Vitro* Growing Controls

MCL cells (Mino CTRL, Mino BM, Mino T, Jeko-1 CTRL, Jeko-1 BM, Jeko-1 S, and Jeko-1 L) were incubated with increasing doses of selected cytotoxic agents (cisplatin and cytarabine). Mino BM cells were more sensitive to cisplatin and cytarabine (approximately twofold) than CTRL Mino

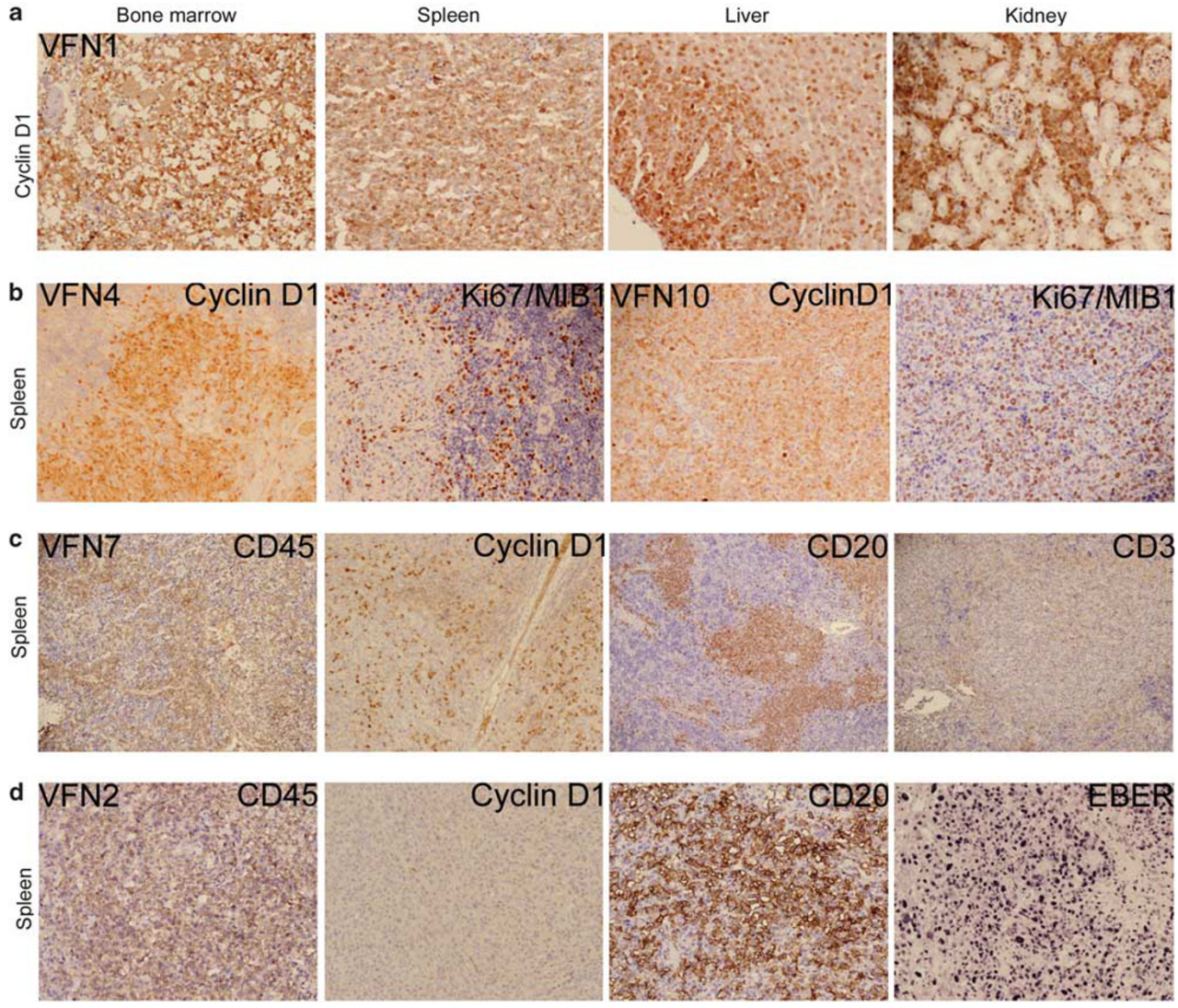

Figure 1 Engraftment of primary mantle cell lymphoma (MCL) cells in NOD-SCID-gamma (NSG) mice. (**a**) Immunohistochemical (IHC) analysis of murine tissues showing diffuse infiltration with cyclin D1+ primary MCL cells obtained from peripheral blood of the patient (VFN-1) with relapsed/refractory disease in transformation to blastoid variant MCL. (**b**) IHC analysis (cyclin D1 and Ki-67) of murine spleen showing engraftment of primary MCL cells (VFN-4 and VFN-10) in NSG mice. (**c**) Xenotransplantation of VFN-7 primary MCL cells resulted in splenic engraftment of CD45+ cells, composed of cyclin D1+ cells, CD20+/cyclin D1-negative cells, and CD3+ cells. (**d**) Xenotransplantation of VFN-2 primary MCL cells resulted in splenic engraftment of CD45+/cyclin D1−/CD20+/EBER+ cells. Original magnification ×200.

cells (Supplementary Figure 3). There were no differences in the sensitivity to cisplatin or cytarabine between T and CTRL Mino cells (data not shown). Jeko-1 BM cells were more sensitive to cisplatin (approximately twofold) and cytarabine (approximately fourfold) than CTRL Jeko-1 cells (Supplementary Figure 3). Jeko-1 S cells were more sensitive to cisplatin (approximately twofold), but not to cytarabine, compared with CTRL Jeko-1 cells (data not shown). There were no differences in the sensitivity to cisplatin or cytarabine between L and CTRL Jeko-1 cells (data not shown).

Secondary Recipients Xenografted with MCL Cells Obtained *Ex Vivo* from the Bone Marrow of Primary Recipients have Significantly Shorter OS Compared with Mice Xenografted with CTRL Cells

On the basis of the results obtained from the microarray and flow cytometry experiments, we assumed that MCL cells growing *in vivo* display complex changes of GEP and immunophenotype, and that those changes may reflect the MCL cell adaptation to the murine microenvironment. We thus decided to test the ability of the *ex vivo* obtained MCL cells to re-engraft into secondary recipients and to evaluate

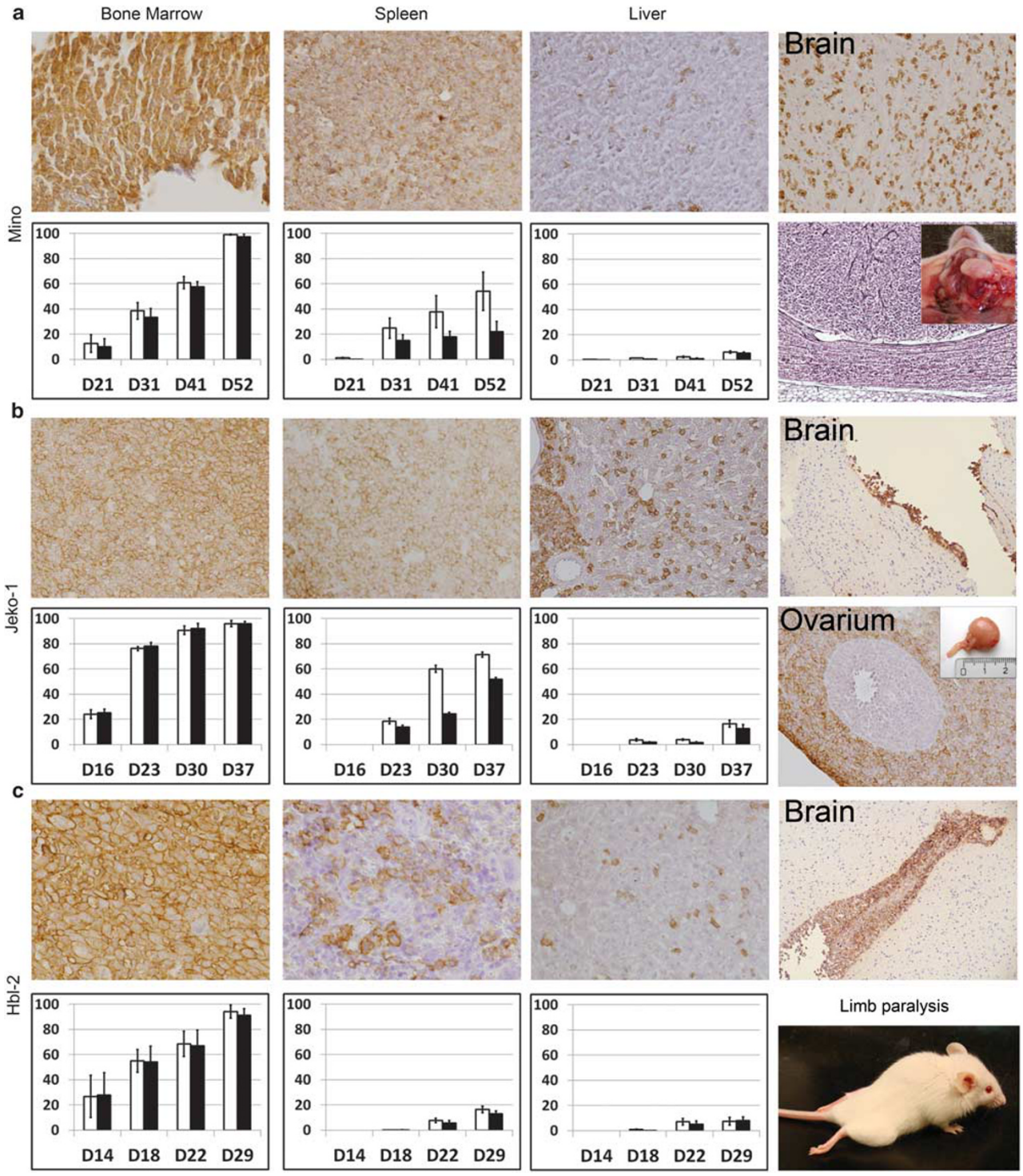

Figure 2 Engraftment of Mino (**a**), Jeko-1 (**b**), and Hbl-2 (**c**) cells in NOD-SCID-gamma (NSG) mice. Immunohistochemical (IHC) analysis of murine bone marrow (BM), spleen, liver, and brain with anti-human CD20 Ab at T4 time point, and the percent infiltration of murine BM, spleen, liver with mantle cell lymphoma (MCL) cells at T1–T4 time points for each cell line (**a**–**c**) are shown (IHC analysis with anti-human CD20 (white columns) and Ki-67 (black columns)). Cell line-specific features of engraftment are also shown: (**a**) A lymph node-like tumor in the left submandibulary region of a Mino-xenografted mouse at T4 time point. Gömöri impregnation revealed collagen 3-rich lymph node-like structures composed predominantly of human MCL B cells. (**b**) An enlarged ovary of Jeko-1-xenografted mouse at T4. IHC analysis (anti-human CD20) showing human MCL cells embedded in the spinocellular tissue with no signs of invasion into the ovarian follicles. (**c**) Typical preterminal hint-leg paralysis of a Hbl-2-xenografted mouse at T4. Original magnification $\times 200$.

Table 2 Engraftment of MCL cell lines in NSG mice

	T1	T2	T3	T4
(a) Percent infiltration of murine tissues with MCL cells (BM, spleen, and liver) at T1–T4 time points				
Mino				
BM	12.7 ± 7	38.6 ± 6.6	61.0 ± 4.8	99.1 ± 0.2
Spleen	1.4 ± 0.2	24.9 ± 8	38.0 ± 12.6	54.2 ± 15.2
Liver	0.6 ± 0.1	1.6 ± 0.1	2.4 ± 0.6	6.3 ± 0.9
Jeko-1				
BM	24.1 ± 3.6	76.3 ± 1.6	90.8 ± 3.3	96.0 ± 2.5
Spleen	0	18.7 ± 2.1	60.2 ± 2.7	71.5 ± 2.1
Liver	0	3.8 ± 1	3.9 ± 0.6	16.7 ± 2.8
Hbl-2				
BM	26.9 ± 16.9	55.0 ± 9.0	68.6 ± 10.1	94.1 ± 5.2
Spleen	0	0.2 ± 0.1	7.7 ± 1.7	16.5 ± 2.7
Liver	0	1.0 ± 0.5	7.2 ± 2.7	7.6 ± 3.0
Granta-519				
BM	4.3 ± 3.9	18.7 ± 9.0	33.9 ± 8.1	62.1 ± 16.2
Spleen	0.1 ± 0	0.8 ± 0.3	18.7 ± 9.7	41.1 ± 11.7
Liver	0.9 ± 0.4	12.3 ± 4.1	38.9 ± 11.5	51.7 ± 12.9
Rec-1				
BM	34.9 ± 2.9	45.2 ± 3.2	57.0 ± 2.9	59.0 ± 6.3
Spleen	12.8 ± 2.0	20.5 ± 2.6	46.7 ± 4.1	47.7 ± 3.9
Liver	0	9.8 ± 0.9	28.4 ± 3.0	40.1 ± 5.4

(b) Percent infiltration of murine kidneys and peripheral blood with MCL cells at T4. Weights of the murine spleen and liver of control mice (Ctrl) and MCL-xenografted mice at T4

	Kidney	*PB*	*Spleen (m/mg)*	*Liver (m/mg)*
Mino	26.9 ± 6.8	0	332 ± 55	1256 ± 249
Jeko-1	5.2 ± 3.5	2.2 ± 0.9	406 ± 36	1711 ± 268
Hbl-2	2 ± 1.5	1.2 ± 1	27 ± 2	733 ± 131
Granta-519	10.5 ± 6.9	12.7 ± 0.1	66 ± 8	3646 ± 75
Rec-1	0.5 ± 0.1	0	178 ± 92	2443 ± 706
Ctrl mice ($n = 3$)			38 ± 17	891 ± 38

Abbreviations: BM, bone marrow; MCL, mantle cell lymphoma; NSG, NOD-SCID-gamma; PB, peripheral blood.

changes in disease behavior. Of interest, the OS of secondary recipient NSG mice xenografted with 0.5×10^6 Mino BM cells was shorter than secondary recipients inoculated with Mino CTRL cells (65.2 ± 3.6 *vs* 84 ± 8 and days, respectively ($P < 0.001$)) (Supplementary Figure 4). Similarly, the OS of secondary recipients inoculated with 0.8×10^6 Jeko-1 CTRL was 41.2 ± 2.6 *vs* 33.8 ± 2.8 for secondary recipients of Jeko-1 BM cells ($P < 0.001$; Supplementary Figure 4).

Experimental Therapy of MCL-Xenografted Mice

The established *in vivo* models of MCL, both cell line-based (Mino- and Jeko-1-xenografted mice) and primary cell-based

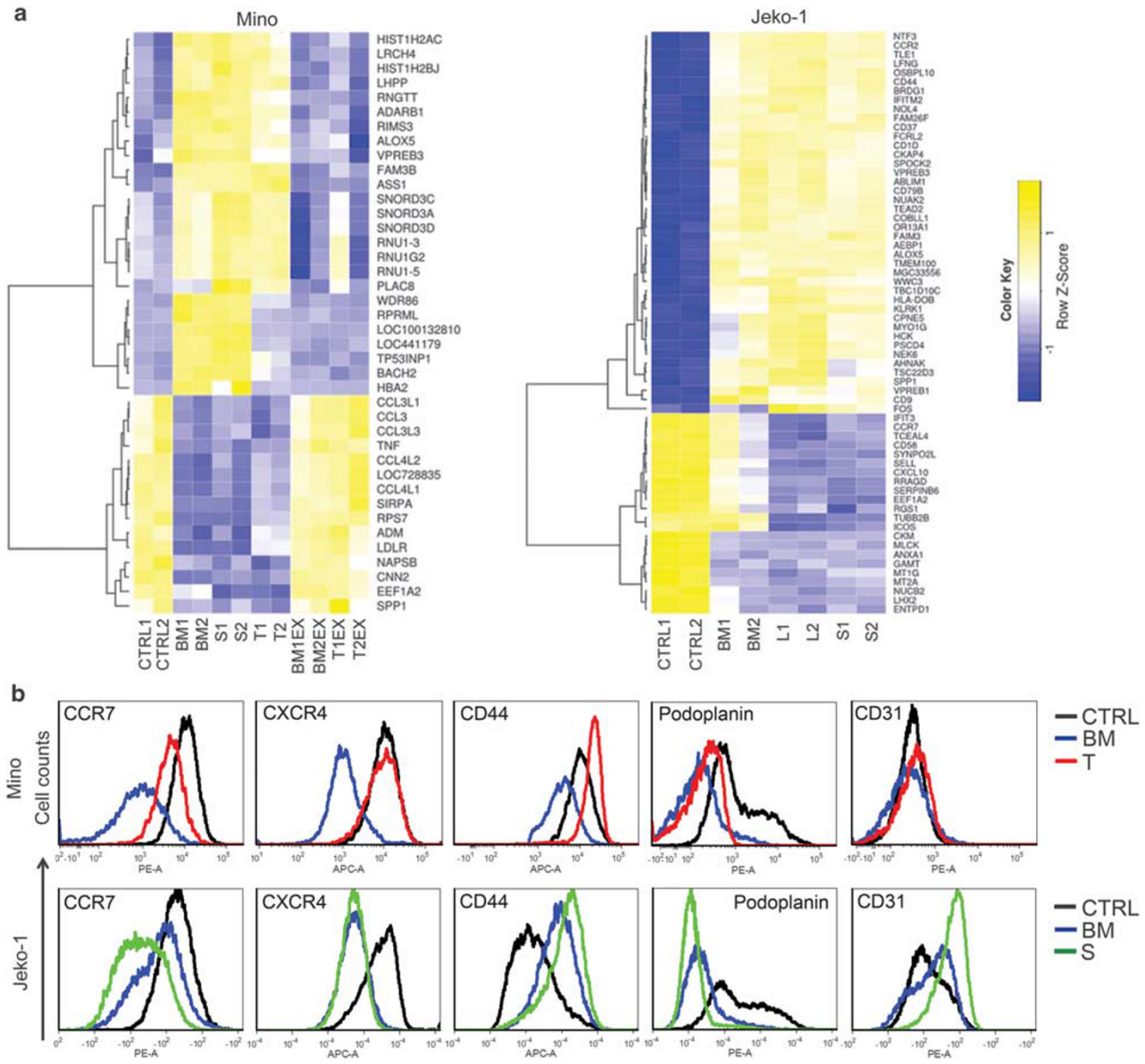

Figure 3 Phenotypic differences between mantle cell lymphoma (MCL) cells obtained *ex vivo* from murine tissues compared with *in vitro* growing controls. (**a**) The most differently expressed genes of MCL cells obtained *ex vivo* from different murine organs: bone marrow (BM), spleen (S), liver (L), and lymph node-like tumors (T) of Mino- and Jeko-1-bearing mice compared with *in vitro* growing controls (CTRL). Gene expression signature of *ex vivo* obtained Mino cells (left) cultured for 14 days *in vitro* reverts to the original *in vitro* signature. (**b**) Flow cytometry analysis of MCL cells obtained *ex vivo* from different murine organs (BM, S, and T) compared with CTRL cells.

(NEMO-bearing mice) were used as tools for the preclinical assessment of experimental therapeutic approaches. Apart from the standardly used chemotherapy drugs (fludarabine, gemcitabine, and bortezomib), the mice were treated with agents, the antitumor activity of which cannot be reliably evaluated *in vitro* including monoclonal antibodies (rituximab and bevacizumab), pro-drugs (cyclophosphamide), cell signaling inhibitors (temsirolimus), or immunomodulatory agents (lenalidomide). *In vivo* treatment of MCL inoculated NSG mice with gemcitabine (Gem), temsirolimus (Tem), cyclophosphamide (Cyc), and rituximab (Rit) significantly prolonged OS in all three tested xenograft models ($P<0.05$). Fludarabine (Flu) significantly prolonged OS in Jeko-1 and Mino ($P<0.05$), but not in NEMO-xenografted mice. Bevacizumab (Bev) significantly ($P<0.05$) prolonged OS in Jeko-1 and NEMO, but not in Mino-xenografted mice. Lenalidomide (Len) significantly prolonged OS only in NEMO-bearing mice, whereas bortezomib (Bor) failed to prolong OS in any of the three tested mouse models at the dose/schedule tested (Figure 4).

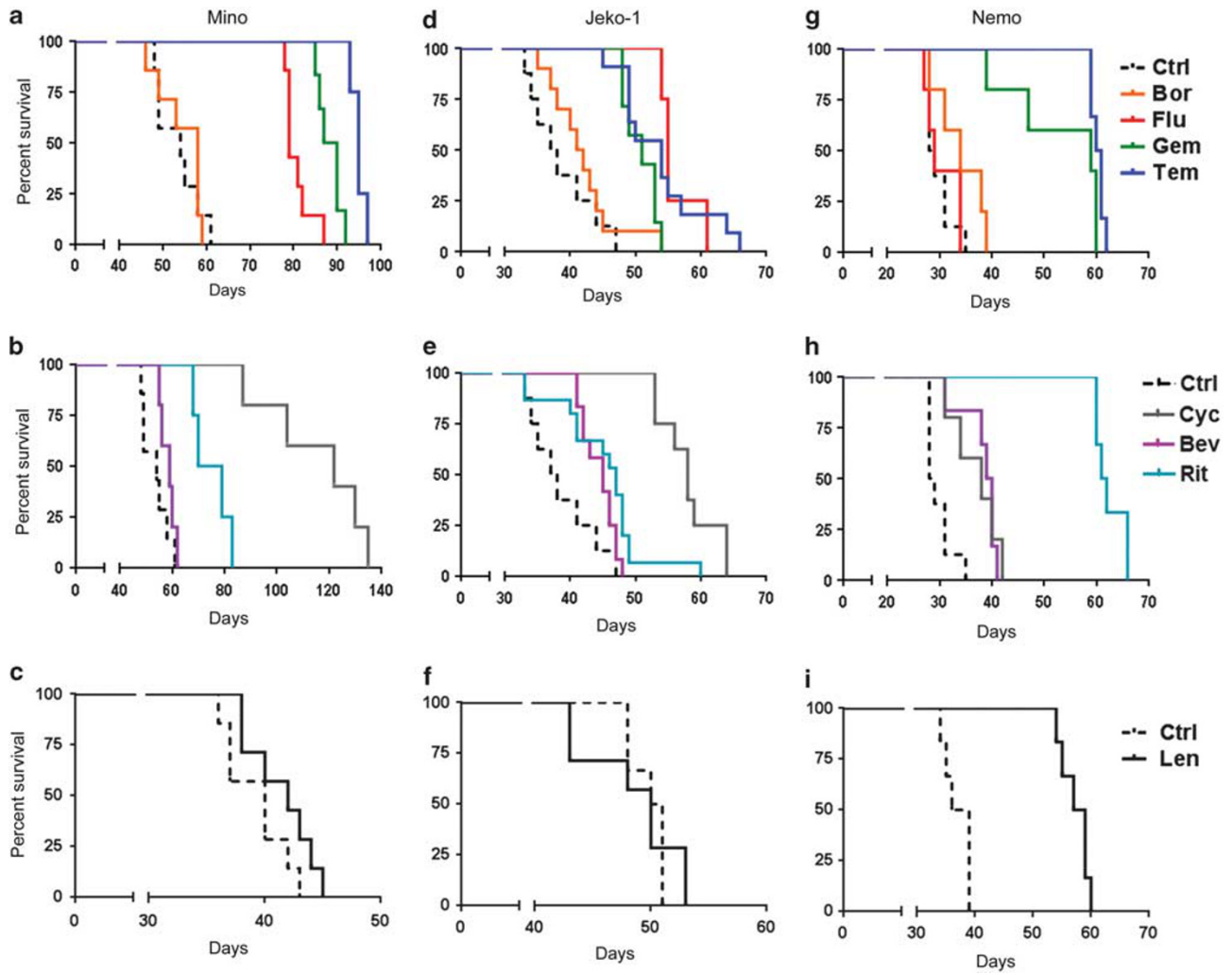

Figure 4 Experimental therapy of xenografted mice. Kaplan–Meier survival curves showing overall survival (OS) of individual treatment cohorts (five to eight animals per cohort) of Mino (**a–c**), Jeko-1 (**d–f**), and Nemo (**g–i**) xenografted mice compared with untreated controls (Ctrl). Gemcitabin (Gem), Temsirolimus (Tem), Cyclophosphamide (Cyc), and Rituximab (Rit) significantly prolonged OS in all Mino (**a**, **b**), Jeko-1 (**d**, **e**), and Nemo (**g**, **h**) xenografted mice ($P<0.05$). Bevacizumab (Bev) significantly ($P<0.05$) prolonged OS in Jeko-1 (**e**) and Nemo (**h**), but not in Mino (**b**), xenografted mice. Fludarabin (Flu) significantly ($P<0.05$) prolonged OS in Mino (**a**) and Jeko-1 (**d**), but not in Nemo (**g**) xenografted mice. Bortezomib (Bor) failed to prolong OS in all MCL-bearing mice (**a**, **d**, **g**). Lenalidomide (Len) significantly ($P<0.05$) prolonged OS in Nemo-xenografted mice (**i**) and failed to prolong OS in both Mino- (**c**) and Jeko-1 (**f**)-xenografted mice. Pooled data of two independent experiments are shown.

DISCUSSION

We established and characterized several metastatic mouse models of human MCL using both primary cells and established cell lines. We first demonstrated that primary MCL cells could engraft in the irradiated NSG mice (Figures 1a and b). Apart from the engraftment of predominantly cyclin D1+ cells (VFN-1, VFN-4, and VFN-10), more complex patterns were observed, including engraftments composed of cyclin D1+, CD20+, and CD3+ cells (VFN-3, VFN-6, VFN-7, and VFN-8). Importantly, in as many as three cases (VFN-2, VFN-11, and VFN-12) injection of primary MCL cells resulted in the engraftment of EBV+ B-cell clones. In general, mouse models of human MCL using primary cells are feasible; however, they are associated with unreliable engraftment and require IHC to confirm engraftment of cyclin D1+ cells, and exclude engraftment of EBV+ B-cell clones or non-MCL cells (for example, T cells). We also demonstrated that in occasional cases (VFN-1) the engrafted primary MCL cells can be harvested (ideally from the enlarged spleen) and either frozen or directly used for re-transplantation into secondary recipients.

Despite the fact that selected primary MCL cells do engraft in immunodeficient NSG mice, it must be taken in mind that most of the currently published preclinical therapies are carried out using established MCL cell line xenografts, usually after subcutaneous injection, whereas i.v. xenotransplantations are less frequently used. In addition, little is

known about the way of engraftment and/or spread of the lymphoma cells in the murine organism upon xeno-transplantation, or about their potential phenotype changes induced by murine microenvironment.

In this study we thoroughly characterized engraftments of five widely used MCL cell lines (Mino, Jeko-1, Granta-519, Hbl-2, and Rec-1) in the immunodeficient NSG mice. In contrast to primary MCL cells, the engraftment of which occurred almost exclusively in the spleen, the principal site of engraftment of all MCL cell lines appeared to be the BM, from where MCL cells apparently disseminated to the spleen, liver, and later in the course of disease to other murine organs and tissues, including the CNS and kidneys. Involvement of other organs, including ovaries, lymph nodes, or PB, appeared to be MCL cell line-specific. The median OS of mice xenografted with MCL cells ranged from 22 ± 1 to 54 ± 3 days. By far, the most biologically aggressive MCL cell line was Granta-519, despite the fact that it demonstrated the slowest proliferation rate *in vitro* of all five MCL cell lines (data not shown). The reason for the observed diversity in the biological aggressiveness of the five MCL cell lines remained largely elusive.

Interestingly, GEP and flow cytometry experiments unveiled that MCL cells growing *in vivo* in different murine organs had different gene expression signatures and immunophenotypes (*in vivo* signature) compared with *in vitro* growing MCL cells (*in vitro* signature). Genes coding for chemokines and chemokine receptors, including CXCL10, CCL3, CCL3L3, CCL4L1, CCL4L2, CXCR4, or CCR7, belonged to the most deregulated genes in MCL cells *in vivo* compared with cells *in vitro*. These results highlight the influence of the tumor microenvironment to the biology of MCL. 'Oxidative phosphorylation' and 'B-cell receptor signaling' belonged to the most downregulated and upregulated functional clusters, respectively. We assume that upon engraftment, MCL cells undergo complex changes of gene and protein expression as a result of adaptation to the microenvironment of murine tissues, including cell–cell interactions, hypoxia, lack of nutrients, engagement of integrin receptors and so on. Not surprisingly, mice re-transplanted from primary to secondary mouse recipients had significantly shorter OS compared with mice xenografted with CTRL cells.

Finally, we confirmed that the mouse models could be used for preclinical assessment of current or novel therapies. Curiously, we noticed a marked difference between the tested *in vitro* sensitivity of MCL cells to some anticancer agents and rather poor outcome when using the same agent for the *in vivo* therapy of MCL-xenografted mice. For example, the *in vitro* lethal dose (LD100) of Jeko-1 cells to gemcitabine and bortezomib was 10 and 16 nM, respectively. Despite the excellent *in vitro* sensitivity to both agents, bortezomib therapy of Jeko-1-xenografted mice failed to improve OS, whereas therapy with high doses of gemcitabine did not lead to eradication of the lymphoma. We suppose that the observed discrepancy between *in vitro* sensitivity (excellent) and *in vivo* efficacy (poor) of many of the tested cytotoxic agents could be explained by the phenotypic changes associated with the engraftment and described in detail above. We also observed that immunomodulatory agent lenalidomide, the anticancer activity of which is based on the modulation of complex interactions of lymphoma cells with the microenvironment, failed to prolong survival of MCL cell line-xenografted mice (Mino and Jeko-1), but significantly prolonged survival of NEMO-bearing mice. In sharp contrast to Jeko-1 and Mino cells, NEMO cells (derived from VFN-1 patient sample) underwent rapid apoptosis upon *ex vivo* culture (after isolation from the infiltrated murine spleen), which clearly emphasizes the continuous dependence of NEMO cells on murine microenvironment for survival (data not shown). We suppose that targeted disruption of these pro-survival bonds by lenalidomide might be responsible for the observed prolongation of OS of NEMO-bearing mice. NEMO-xenografted mice thus represent an appropriate *in vivo* system for the study of lenalidomide biology.

In conclusion, we established and characterized several mouse models of human MCL using both primary MCL cells and MCL cell lines. We demonstrated that the engrafted MCL cells are biologically distinct populations because they display complex changes in gene expression, immunophenotype, and sensitivity to cytotoxic agents compared with *in vitro* growing MCL cell lines. These findings may have extensive implications for preclinical research.

Supplementary Information accompanies the paper on the Laboratory Investigation website (http://www.laboratoryinvestigation.org)

ACKNOWLEDGMENTS

We to Gabriela Spanila and Miluse Kreidlova for quantitative analysis of EBV DNA. All *in vivo* experiments were performed at the Centre for Experimental Biomodels, First Faculty of Medicine, Charles University in Prague. This study was supported by IGA-MZ NT13201-4/2012, UNCE 204021, PRVOUK P24/LF1/3, PRVOUK 27/LF1/1, GACR P302/12/G157/1, GAUK 446211.

DISCLOSURE/CONFLICT OF INTEREST

The authors declare no conflict of interest.

1. Bosch F, Jares P, Campo E, *et al.* PRAD-1/cyclin D1 gene overexpression in chronic lymphoproliferative disorders: a highly specific marker of mantle cell lymphoma. Blood 1994;84:2726–2732.
2. Pinyol M, Hernandez L, Cazorla M, *et al.* Deletions and loss of expression of p16INK4a and p21Waf1 genes are associated with aggressive variants of mantle cell lymphomas. Blood 1997;89:272–280.
3. Hernandez L, Bea S, Pinyol M, *et al.* CDK4 and MDM2 gene alterations mainly occur in highly proliferative and aggressive mantle cell lymphomas with wild-type INK4a/ARF locus. Cancer Res 2005;65:2199–2206.
4. Camacho E, Hernandez L, Hernandez S, *et al.* ATM gene inactivation in mantle cell lymphoma mainly occurs by truncating mutations and missense mutations involving the phosphatidylinositol-3 kinase domain and is associated with increasing numbers of chromosomal imbalances. Blood 2002;99:238–244.

5. Greiner TC, Moynihan MJ, Chan WC, *et al.* p53 mutations in mantle cell lymphoma are associated with variant cytology and predict a poor prognosis. Blood 1996;87:4302–4310.
6. Lenz G, Dreyling M, Hiddemann W. Mantle cell lymphoma: established therapeutic options and future directions. Ann Hematol 2004;83: 71–77.
7. Weisenburger DD, Vose JM, Greiner TC, *et al.* Mantle cell lymphoma. A clinicopathologic study of 68 cases from the Nebraska Lymphoma Study Group. Am J Hematol 2000;64:190–196.
8. Ford RJ, Shen L, Lin-Lee YC, *et al.* Development of a murine model for blastoid variant mantle-cell lymphoma. Blood 2007;109:4899–4906.
9. Vincent-Fabert C, Fiancette R, Rouaud P, *et al.* A defect of the INK4-Cdk4 checkpoint and Myc collaborate in blastoid mantle cell lymphoma-like lymphoma formation in mice. Am J Pathol 2012;180:1688–1701.
10. Smith MR, Joshi I, Jin F, *et al.* Murine model for mantle cell lymphoma. Leukemia 2006;20:891–893.
11. Wang M, Zhang L, Han X, *et al.* A severe combined immunodeficient-hu in vivo mouse model of human primary mantle cell lymphoma. Clin Cancer Res 2008;14:2154–2160.
12. Rolland D, Camara-Clayette V, Barbarat A, *et al.* Farnesyltransferase inhibitor R115777 inhibits cell growth and induces apoptosis in mantle cell lymphoma. Cancer Chemother Pharmacol 2008;61:855–863.
13. Gupta M, Hendrickson AE, Yun SS, *et al.* Dual mTORC1/mTORC2 inhibition diminishes Akt activation and induces Puma-dependent apoptosis in lymphoid malignancies. Blood 2012;119:476–487.
14. Jones RJ, Baladandayuthapani V, Neelapu S, *et al.* HDM-2 inhibition suppresses expression of ribonucleotide reductase subunit M2, and synergistically enhances gemcitabine-induced cytotoxicity in mantle cell lymphoma. Blood 2011;118:4140–4149.
15. Mahadevan D, Stejskal A, Cooke LS, *et al.* Aurora A inhibitor (MLN8237) plus vincristine plus rituximab is synthetic lethal and a potential curative therapy in aggressive B-cell non-Hodgkin lymphoma. Clin Cancer Res 2012;18:2210–2219.
16. Gomori G. Silver impregnation of reticulum in paraffin sections. Am J Pathol 1937;13:993–1002 5.
17. Team RDC. R: a language and environment for statistical computing: R Foundation for Statistical Computing 2011) (ISBN 3–900051–07–0).
18. Bioinformatics and Computational Biology Solutions Using R and Bioconductor. 2005; Accessed at http://www.springerlink.com/content/g26110k024423738/.
19. Dunning MJ, Smith ML, Ritchie ME, *et al.* beadarray: R classes and methods for Illumina bead-based data. Bioinformatics 2007;23: 2183–2184.